15TH IEA HEAT PUMP CONFERENCE
MAY 26–29, 2026 | HOFBURG
VIENNA 2026
DECARBONISATION THROUGH INNOVATION

High-order finite line source solution for the simulation of straight geothermal boreholes

Massimo Cimmino[a,*], Alberto Lazzarotto[b]

[a]Polytechnique Montréal, Département de génie mécanique, Montréal, Québec, Canada
[b]KTH Royal Institute of Technology, Department of Energy Technology, Division of Applied Thermodynamics and Refrigeration, Stockholm, Sweden

Abstract

The finite line source solution is routinely used for thermal simulations of geothermal boreholes, for instance in the evaluation of g-functions. This solution models thermal response factors that give the ground temperature variation due to heat extraction at a borehole and is the fundamental building block for borehole simulations based on semi-analytical methods. In typical approaches, piecewise-uniform heat transfer rates are assumed along boreholes and the resulting temperature variations are averaged along borehole segments. Recently, a simulation method that assumes piecewise-polynomial heat transfer rates along the borehole was introduced. Temperature variations are evaluated at nodes along the boreholes, instead of averaged along segments, facilitating the formulation of the finite line source solution. In this paper, a specialized high-order finite line source solution is developed for straight boreholes, including vertical and inclined boreholes. A recurrence formula is presented to evaluate higher order solutions from the zeroth and first order solutions, with only the zeroth order solution necessitating the numerical evaluation of an integral. Compared to earlier methods, the new solution decreases the number of integral evaluations to one evaluation per ground temperature from a number equal to the number of state variables (i.e. number of discrete values of heat extraction rates) per ground temperature. While the specialized solution correctly evaluates high-order finite line source solutions, it is shown that numerical errors are amplified when using the recurrence formula.

Keywords: Ground-source heat pumps; Geothermal boreholes; Finite line source solution.

1. Introduction

Thermal simulations of ground-source heat pump systems aim to predict the variations of the heat carrier fluid temperatures in the geothermal borefield. A heat transfer model of the geothermal boreholes and the ground is employed to evaluate the evolution of ground temperatures – typically evaluated at the borehole walls – due to heat injection or extraction during the operation of the system. A common approach is to temporally and spatially superimpose analytical heat source solutions to obtain temperature variations along the boreholes, and then consider the effective borehole thermal resistance to retrieve the heat carrier fluid temperature.

Assuming that pure conduction prevails in a ground with isotropic and homogeneous thermal properties and with a constant and uniform temperature at the ground surface, the finite line source analytical solution can be used to evaluate ground temperature variations by modelling boreholes as line sources [1, 2]. Making use of averaged temperature variations along line segments [3, 4] and assuming piecewise-uniform heat transfer rates along the boreholes, boreholes can be discretized to apply different boundary conditions along the boreholes, such as a uniform borehole wall temperature [5], an equal inlet fluid temperature in parallel-connected boreholes [6], or a uniform fluid temperature inside boreholes [7]. The approach also applies when

* Corresponding author. Tel.: +1-514-340-4711 (4894)
E-mail address: massimo.cimmino@polymtl.ca

15th IEA Heat Pump Conference 2026 - IGS3.1 - https://doi.org/10.23697/3554-gt71

boreholes are inclined [8], although it necessitates specialized *inclined* finite line source solutions [9–11]. Despite not being covered here, accelerated approaches to evaluate ground temperatures have been proposed for vertical boreholes and extensions of the finite line source solutions have been proposed to model, for instance, groundwater advection and heterogeneous ground properties.

Recently, a discretization approach assuming piecewise-polynomial variations of heat transfer rates and borehole wall temperatures was developed [12]. The new approach presents the advantage that borehole wall temperatures are evaluated at nodes along the boreholes, rather than averaged along line segments. This makes the formulation of the finite line source solution simpler and applicable to vertical, inclined and curved boreholes. In addition, the solutions for vertical and inclined boreholes are the same, thus avoiding the need for a specialized solution in the latter case. Gains in accuracy have also been shown. The approach necessitates, for each point where the temperature is to be evaluated, the solution of one integral per discretization node along the borehole. This is similar to the averaged temperature approach, where one integral is solved per line segment. In both cases, one integral is required per state variable along the borehole.

In this paper, a specialized solution is developed for piecewise-polynomial heat transfer rates along straight boreholes. The high-order finite line source solution is first defined. A recurrence formula is derived to evaluate higher-order solutions from the zeroth and first orders. Thermal response factors for temperature variations at points due to the contribution of each node along the borehole are then evaluated from the finite line source solutions. The new specialized solution decreases the number of required integral evaluations per evaluation point down to 1 (from a number equal to the number of nodes along the borehole).

2. Methodology

The borehole is modelled as a straight finite line source, as shown on Fig. 1. The borehole has a length L. Its top end is located at a position $\vec{p}_0 = (x_0, y_0, z_0)$ in ground of thermal conductivity λ and thermal diffusivity α. Its axis is oriented following the unit vector $\vec{u}$. Note that the z-axis is oriented upwards. The coordinate along the borehole $\xi \in [-1,\ 1]$ is centered at the borehole mid-point (i.e. at $\xi = 0$). Quantities, such as the position $\vec{p}_b(\xi)$ and longitudinal position $s_b(\xi)$ along the borehole can be expressed as a function of this coordinate:

$$\vec{p}_b(\xi) = \vec{p}_0 + \frac{\vec{u}L}{2}(1+\xi), \tag{1}$$

$$s_b(\xi) = \frac{L}{2}(1+\xi). \tag{2}$$

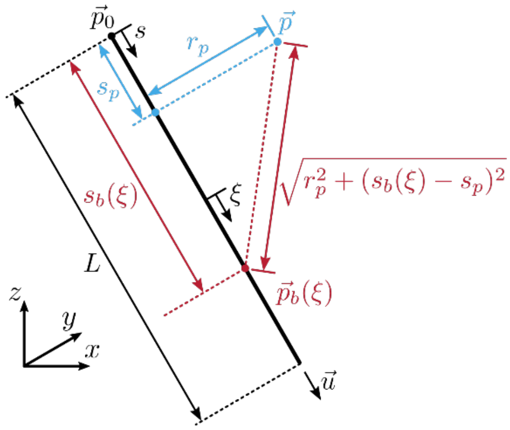

Figure 1. Geometry of the finite line source

2.1. High-order finite line source solution

The temperature drop at a point $\vec{p}$ around the line source is evaluated by the integration of the point heat source solution, weighted by the heat extraction rate per unit borehole length $q'(\xi)$ (constant in time but varying along the length of the line), along the length of the line (i.e. from $\xi = -1$ to 1):

$$\Delta T^{+}(\vec{p},t) = \frac{1}{2\pi\lambda}\int_{1/\sqrt{4\alpha t}}^{\infty} \exp\left(-r_p^2 u^2\right) \cdot \frac{L}{2\sqrt{\pi}}\int_{-1}^{1} q'(\xi) \exp\left(-\left(s_b(\xi) - s_p\right)^2 u^2\right) d\xi \, du, \tag{4}$$

where $\Delta T^{+}(\vec{p},t)$ is the temperature drop at point $\vec{p}$ due to a constant (but varying along the length) heat extraction starting at time 0 and maintained until time t, r_p is the radial distance between the axis of the borehole and point $\vec{p}$, and s_p is the longitudinal projection of point $\vec{p}$ onto the borehole. Note that the integration variable u is distinct from the unit vector $\vec{u}$. The radial-axial position (r_p, s_p) is given by:

$$r_p = \|(\vec{p}_b(\xi) - \vec{p}) \times \vec{u}\|, \tag{5}$$

$$s_p = (\vec{p}_0 - \vec{p}) \cdot \vec{u}, \tag{6}$$

where $(\times)$ denotes the cross product, $(\cdot)$ denotes the dot product and $\|(\;\;)\|$ is the Euclidean norm.

Assuming that the heat extraction rate can be expressed as a polynomial of degree $n-1$:

$$q'(\xi) = a_0 + a_1\xi + a_2\xi^2 + \cdots + a_{n-1}\xi^{n-1}, \tag{7}$$

the temperature drop can be expressed as a weighted sum of solutions corresponding to each order k of the polynomial representation of the heat extraction rate:

$$\begin{aligned}\Delta T^{+}(\vec{p},t) &= \frac{1}{2\pi\lambda}\sum_{k=0}^{n-1} a_k \int_{1/\sqrt{4\alpha t}}^{\infty} \exp\left(-r_p^2 u^2\right) \cdot \frac{L}{2\sqrt{\pi}}\int_{-1}^{1} \xi^k \exp\left(-\left(s_b(\xi) - s_p\right)^2 u^2\right) d\xi \, du \\ &= \frac{1}{2\pi\lambda}\sum_{k=0}^{n-1} a_k I_k(\vec{p},t)\end{aligned}, \tag{8}$$

where $I_k(\vec{p},t)$ is defined as the finite line source solution of order k evaluated at point $\vec{p}$ and at time t.

A change of variable $\eta = (1+\xi) - 2s_p/L$ is introduced to facilitate the solution of the integrals in Eq. (8). The heat extraction rate can be expressed as a function of the new variable η instead of the coordinate ξ using a polynomial of the same degree $n-1$:

$$q'(\eta) = b_0 + b_1\eta + b_2\eta^2 + \cdots + b_{n-1}\eta^{n-1}, \tag{9}$$

and the expression for the temperature drop becomes:

$$\begin{aligned}\Delta T^{+}(\vec{p},t) &= \frac{1}{2\pi\lambda}\sum_{k=0}^{n-1} b_k \int_{1/\sqrt{4\alpha t}}^{\infty} \exp\left(-r_p^2 u^2\right) \cdot \frac{L}{2\sqrt{\pi}}\int_{-2s_p/L}^{2-2s_p/L} \eta^k \exp\left(-\frac{L^2\eta^2u^2}{4}\right) d\eta \, du \\ &= \frac{1}{2\pi\lambda}\sum_{k=0}^{n-1} b_k J_k(\vec{p},t)\end{aligned}, \tag{10}$$

where $J_k(\vec{p},t)$ is the integral of order k. The inner integrals of I_k and J_k result from the integration over the same length corresponding to the interval $\xi = -1$ to 1. The difference between the two resides in the fact that the heat extraction rate is centered around the midpoint of the borehole in the case of I_k (i.e. at $\xi = 0$) and around the projection of point $\vec{p}$ onto the borehole axis in the case of J_k (i.e. at $\eta = 0$).

The finite line source solutions I_k can be evaluated from the integrals J_k using the binomial formula and the variable change between Eqs. (7) and (9):

$$I_{n-1}(\vec{p},t) = \sum_{k=0}^{n-1} \binom{n-1}{k} \left(\frac{2s_p}{L} - 1\right)^{n-k-1} J_k(\vec{p},t). \tag{11}$$

2.2. Zeroth order integral (J_0)

The zeroth order integral of Eq. (10), for $k = 0$, is given by:

$$J_0(\vec{p},t) = \int_{1/\sqrt{4\alpha t}}^{\infty} \exp\left(-r_p^2 u^2\right) \cdot \underbrace{\frac{L}{2\sqrt{\pi}}\int_{-2s_p/L}^{2-2s_p/L} \exp\left(-\frac{L^2\eta^2u^2}{4}\right) d\eta}_{X_0(\vec{p},u)} \, du. \tag{12}$$

The inner integral X_0 has a solution:

$$X_0(\vec{p},u) = \frac{1}{2u}\left[\operatorname{erf}\left(u\left(L - s_p\right)\right) + \operatorname{erf}\left(us_p\right)\right]. \tag{13}$$

The resulting second integral, however, does not have a solution:

$$J_0(\vec{p},t) = \int_{1/\sqrt{4\alpha t}}^{\infty} \exp\left(-r_p^2 u^2\right) \cdot X_0(\vec{p},u)du. \tag{14}$$

2.3. First order integral (J_1)

The first order integral of Eq. (10), for $k = 1$, is given by:

$$J_1(\vec{p},t) = \int_{1/\sqrt{4\alpha t}}^{\infty} \exp\left(-r_p^2 u^2\right) \cdot \underbrace{\frac{L}{2\sqrt{\pi}} \int_{-2s_p/L}^{2-2s_p/L} \eta \exp\left(-\frac{L^2\eta^2u^2}{4}\right) d\eta}_{X_1(\vec{p},u)}\, du. \tag{15}$$

The inner integral X_1 has a solution:

$$X_1(\vec{p},u) = \frac{-1}{u^2\sqrt{\pi}L}\left[\exp\left(-u^2\left(L - s_p\right)^2\right) - \exp\left(-u^2 s_p^2\right)\right], \tag{16}$$

and the resulting second integral also has a solution:

$$\begin{aligned} J_1(\vec{p},t) = \frac{1}{L}&\left[\sqrt{r_p^2 + \left(L - s_p\right)^2}\operatorname{erf}\left(\frac{\sqrt{r_p^2 + \left(L - s_p\right)^2}}{\sqrt{4\alpha t}}\right) + \sqrt{r_p^2 + s_p^2}\operatorname{erf}\left(\frac{\sqrt{r_p^2 + s_p^2}}{\sqrt{4\alpha t}}\right)\right]. \\ &- \frac{\sqrt{4\alpha t}}{\sqrt{\pi}L}\left[\exp\left(-\frac{r_p^2 + \left(L - s_p\right)^2}{4\alpha t}\right) - \exp\left(-\frac{r_p^2 + s_p^2}{4\alpha t}\right)\right] \end{aligned} \tag{17}$$

2.4. High-order integrals (J_k)

2.4.1. Recurrence formula for the inner integrals (X_k)

In the case of higher order integrals, for $k \geq 2$, a recurrence formula can be obtained. The solution involves first obtaining a recurrence formula for the high-order inner integral X_k of J_k, defined by:

$$J_k(\vec{p},t) = \int_{1/\sqrt{4\alpha t}}^{\infty} \exp\left(-r_p^2 u^2\right) \cdot \underbrace{\frac{L}{2\sqrt{\pi}} \int_{-2s_p/L}^{2-2s_p/L} \eta^k \exp\left(-\frac{L^2\eta^2u^2}{4}\right) d\eta}_{X_k(\vec{p},u)}\, du, \tag{18}$$

$$X_k(\vec{p},u) = \frac{L}{2\sqrt{\pi}} \int_{-2s_p/L}^{2-2s_p/L} \eta^k \exp\left(-\frac{L^2\eta^2u^2}{4}\right) d\eta. \tag{19}$$

A useful property of the inner integral relates its derivative to lower orders of the inner integral. Taking the derivative of Eq. (19) with respect to the variable u:

$$\begin{aligned} \frac{dX_k}{du}(\vec{p},u) &= \frac{L}{2\sqrt{\pi}} \int_{-2s_p/L}^{2-2s_p/L} \eta^k \left(-\frac{uL^2\eta^2}{2}\right) \exp\left(-\frac{L^2\eta^2u^2}{4}\right) d\eta \\ &= -\frac{uL^2}{2} X_{k+2}(\vec{p},u) \end{aligned}, \tag{20}$$

with the derivative of the k^{th} order inner integral thus related to the inner integral of order $k + 2$.

The recurrence formula for X_k is obtained by integration by parts, as follows:

$$
\begin{aligned}
X_k(\vec{p},u) &= \frac{L}{2\sqrt{\pi}}\int_{-2s_p/L}^{2-2s_p/L} \underbrace{\eta^{k-1}}_{u'} \cdot \underbrace{\eta \exp\left(-\frac{L^2\eta^2u^2}{4}\right)d\eta}_{dv'} \\
&= \frac{L}{2\sqrt{\pi}}\left(-\frac{2\eta^{k-1}}{u^2L^2}\exp\left(-\frac{L^2\eta^2u^2}{4}\right)\right)_{\eta=-2s_p/L}^{2-2s_p/L} + \underbrace{\frac{L}{2\sqrt{\pi}}\int_{-2s_p/L}^{2-2s_p/L}\frac{2(k-1)}{u^2L^2}\eta^{k-2}\exp\left(-\frac{L^2\eta^2u^2}{4}\right)d\eta}_{\frac{2(k-1)}{u^2L^2}X_{k-2}(\vec{p},u)} \\
&= \frac{-1}{u^2\sqrt{\pi}L}\left(\eta^{k-1}\exp\left(-\frac{L^2\eta^2u^2}{4}\right)\right)_{\eta=-2s_p/L}^{2-2s_p/L} + \frac{2(k-1)}{u^2L^2}X_{k-2}(\vec{p},u)
\end{aligned}
\tag{21}
$$

2.4.2. Recurrence formula for the high-order integrals (J_k)

The recurrence formula is obtained by considering each of the derivative property of Eq. (20) and the recurrence formula of the inner integral of Eq. (21). Inserting the derivative property of Eq. (20) into the high-order integral of Eq. (18) and applying integration by parts:

$$
\begin{aligned}
J_k(\vec{p},t) &= \frac{-2}{L^2}\int_{1/\sqrt{4\alpha t}}^{\infty} \underbrace{\frac{1}{u}\exp\left(-r_p^2u^2\right)}_{u'} \cdot \underbrace{\frac{dX_{k-2}}{du}(\vec{p},u)du}_{dv'} \\
&= -\frac{2}{L^2}\left(\frac{1}{u}\exp\left(-r_p^2u^2\right)X_{k-2}(\vec{p},u)\right)_{u=\frac{1}{\sqrt{4\alpha t}}}^{\infty} - \underbrace{\frac{2}{L^2}\int_{1/\sqrt{4\alpha t}}^{\infty} 2r_p^2\exp\left(-r_p^2u^2\right)\cdot X_{k-2}(\vec{p},u)du}_{\frac{4r_p^2}{L^2}J_{k-2}(\vec{p},t)} \\
&\quad -\frac{2}{L^2}\underbrace{\int_{1/\sqrt{4\alpha t}}^{\infty}\frac{1}{u^2}\exp\left(-r_p^2u^2\right)\cdot X_{k-2}(\vec{p},u)du}_{Y_{k-2}(\vec{p},t)} \\
&= \frac{2}{L^2}\sqrt{4\alpha t}\exp\left(-\frac{r_p^2}{4\alpha t}\right)X_{k-2}\left(\vec{p},\frac{1}{\sqrt{4\alpha t}}\right) - \frac{4r_p^2}{L^2}J_{k-2}(\vec{p},t) - \frac{2}{L^2}Y_{k-2}(\vec{p},t)
\end{aligned}
\tag{22}
$$

This expression includes a new integral Y_{k-2}, which does not have a solution. However, it can be eliminated by considering the recurrence formula of the inner integral. Inserting the recurrence formula of Eq. (21) into Eq. (18):

$$
\begin{aligned}
J_k(\vec{p},t) &= \frac{2(k-1)}{L^2}\underbrace{\int_{1/\sqrt{4\alpha t}}^{\infty}\frac{1}{u^2}\exp\left(-r_p^2u^2\right)\cdot X_{k-2}(\vec{p},u)du}_{Y_{k-2}(\vec{p},t)} \\
&\quad \underbrace{-\frac{1}{\sqrt{\pi}L}\int_{1/\sqrt{4\alpha t}}^{\infty}\frac{1}{u^2}\exp\left(-r_p^2u^2\right)\cdot\left(\eta^{k-1}\exp\left(-\frac{L^2\eta^2u^2}{4}\right)\right)_{\eta=-2s_p/L}^{2-2s_p/L}du.}_{K_{k-1}(\vec{p},t)} \\
&= \frac{2(k-1)}{L^2}Y_{k-2}(\vec{p},t) - K_{k-1}(\vec{p},t)
\end{aligned}
\tag{23}
$$

The integral Y_{k-2} can be isolated in Eq. (23) and substituted into Eq. (22), leading to the final recurrence formula for the high-order integral J_k:

$$
J_k(\vec{p},t) = \frac{2(k-1)}{kL^2}\sqrt{4\alpha t}\exp\left(-\frac{r_p^2}{4\alpha t}\right)X_{k-2}\left(\vec{p},\frac{1}{\sqrt{4\alpha t}}\right) - \frac{4(k-1)r_p^2}{kL^2}J_{k-2}(\vec{p},t) - \frac{1}{k}K_{k-1}(\vec{p},t),
\tag{24}
$$

where the integral K_{k-1} has a solution:

$$
K_{k-1}(\vec{p},t) = \frac{1}{\sqrt{\pi}L}\left[\eta^{k-1}\left(\frac{1}{u}\exp\left(-d^2(\eta)\,u^2\right) - d(\eta)\sqrt{\pi}\,\mathrm{erfc}\left(d(\eta)\,u\right)\right)\right]_{\eta=-2s_p/L}^{2-2s_p/L},
\tag{25}
$$

$$
d(\eta) = \sqrt{r_p^2 + \frac{L^2\eta^2}{4}}.
\tag{26}
$$

It can be seen that the evaluation of integrals J_k up to an order n only involves the evaluation of one integral, that of the zeroth order J_0, which only affects the even numbered orders. The finite line source solutions I_k can then be obtained from Eq. (11). This provides potential computational benefits over the numerical evaluation of the integrals of Eq. (8). While it can be reduced to a single integral (instead of a double integral) by inverting the order of integration, it still leads to the evaluation of n integrals.

2.5. Thermal response factors (h_m)

The superposition of finite line source solutions in Eq. (8) depends on the values of coefficients of the polynomial expression of the heat extraction rate. For simulations or for the evaluation of g-functions, it is more convenient to express thermal response factors based on values of the heat extraction rates at nodes distributed along the finite line source, as proposed by Cimmino et al. [12]. Here, it is considered that n nodes are distributed along the source at coordinates ξ_m corresponding to the locations of the roots of the Legendre polynomial of degree n, as used in Gauss-Legendre quadrature. The temperature drop at a point $\vec{p}$ is then given by:

$$\Delta T(\vec{p},t) = \frac{1}{2\pi\lambda}\sum_{m=0}^{n-1} q'(\xi_m) h_m(\vec{p},t), \tag{27}$$

where $h_m(\vec{p},t)$ is the thermal response factor of node m onto point $\vec{p}$ at a time t and $q'(\xi_m)$ is the heat extraction rate at node m.

The thermal response factor is evaluated from the finite line source solutions. Using the method of images, the finite line sources evaluated at a mirrored point is subtracted:

$$h_m(\vec{p},t) = \sum_{k=0}^{n-1} c_{m,k}\left(I_k(\vec{p},t) - I_k(\hat{\vec{p}},t)\right), \tag{28}$$

where $\hat{\vec{p}} = (x,y,-z)$ is the mirrored point with regards to the horizontal ground surface ($z = 0$). The coefficients $c_{m,k}$ only depend on the locations of the nodes [12]:

$$\left[c_{m,k}\right] = \begin{bmatrix} 1 & 1 & \cdots & 1 \\ \xi_0 & \xi_1 & \cdots & \xi_{n-1} \\ \xi_0^2 & \xi_1^2 & \cdots & \xi_{n-1} \\ \vdots & \vdots & & \vdots \\ \xi_0^{n-1} & \xi_1^{n-1} & \cdots & \xi_{n-1}^{n-1} \end{bmatrix}^{-1}. \tag{29}$$

3. Results

The accuracy of the proposed expressions is evaluated for the case of a single vertical borehole of length L = 150 m and radius r_b = 0.075 m, buried at a distance D = 4 m from the ground surface. The ground has a thermal conductivity λ = 2 W/m·K and a thermal diffusivity α = 10^{-6} m^2/s. The discretization of the borehole employs 11 nodes, and thus the first eleven orders (from k = 0 to k = 10) of the integrals and finite line source solutions are considered. The expressions are evaluated at time values corresponding to the dimensionless range $\ln(t/t_s)$ = -5 to 5 (with $t_s = L^2/9\alpha$), which covers the time scales of interest for the evaluation of long-term thermal response factors. The methodology is implemented in Python using `numpy` [13] and `scipy` [14].

3.1. Inner integrals (X_k)

Fig. 2 shows the values of the 0th, 1st, 9th and 10th order of the inner integral X_k evaluated at the borehole mid-point (i.e. at $r_p = r_b$ and $s_p = L/2$) using the recurrence formula of Eq. (21) along with the solutions of the first two orders in Eqs. (13) and (16). Values are shown as a function of the integration variable $u = 1/\sqrt{4\alpha t}$, and thus large values of time correspond to small values of u. The absolute error $|\varepsilon|$ is evaluated with respect to reference values obtained from the numerical integration of Eq. (19) using adaptive 21-point Gauss-Konrod quadrature as implemented in `scipy.integrate.quad_vec`. It is shown that the absolute error increases at higher orders and at low values of u, reaching $|\varepsilon|$ = 0.193 when k = 10 and u = $8.21\cdot10^{-4}$ (corresponding to $\ln(t/t_s)$ = 5). The amplification of the error is explained by the factor $1/u^2L^2$ that appears in the recurrence formula of Eq. (21). Unrolling the formula, this leads to factors up to $1/(uL)^k$. At $\ln(t/t_s)$ = 5, the factor $(uL)^k = 18.27^k$ varies from unity (at $k = 0$) to the order of 10^{12} (at $k = 10$). Since low values of u generate the largest errors, the rest of the analysis will focus on the case when $\ln(t/t_s)$ = 5.

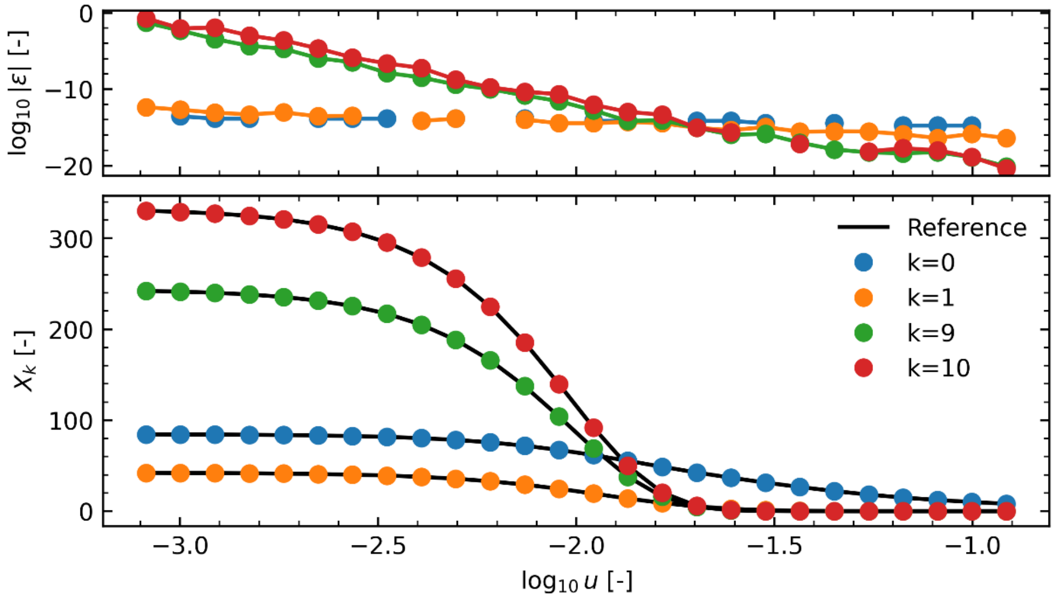

Figure 2. Inner integrals X_k evaluated at the mid-point of the borehole at $r_p = r_b$: (top) absolute errors, and (bottom) values

3.2. High-order integrals (J_k)

Fig. 3 shows the values of the 0th, 1st, 9th and 10th order of the integral J_k evaluated along the borehole (i.e. at $r_p = r_b$) using the recurrence formula of Eq. (24) along with the solutions of the first two orders in Eqs. (14) and (17). The 0th order integral and reference values of the integral are evaluated using the same aforementioned adaptive 21-point Gauss-Konrod quadrature. Here again, the absolute error increases at higher orders. The absolute error at the borehole mid-point is $|\varepsilon| = 5.82{\cdot}10^{-5}$ when $k = 10$ and $J_{10} = 0.0936$. The recurrence formula for the integral J_k involves a factor $-r_p^2/L^2$. Since r_b is generally much lower than L, the factor is much smaller than 1 at the borehole wall. Numerical errors may still arise due to alternating signs of successive terms. Further from the borehole, r_p can grow to the same order as L. Fig. 4 shows the values of the 0th, 1st, 9th and 10th order of the integral J_k evaluated at a distance $r_p = L$ from the borehole. The absolute error and the integral are of the same order as at $r_p = r_b$: the maximum absolute error is $|\varepsilon| = 5.71{\cdot}10^{-5}$ at the mid-point when $k = 10$ and $J_{10} = 0.0349$. The relative errors $|\varepsilon|/J_{10}$ are thus $6.22{\cdot}10^{-4}$ and $1.63{\cdot}10^{-3}$ at $r_p = r_b$ and $r_p = L$.

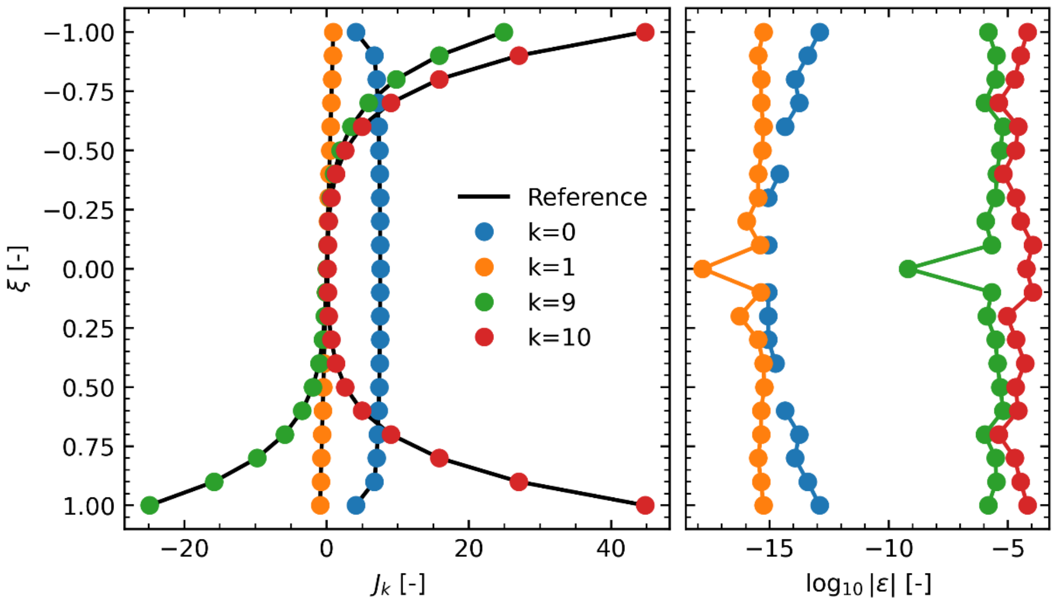

Figure 3. High-order integrals J_k evaluated along the borehole at $r_p = r_b$: (left) values, and (right) absolute errors

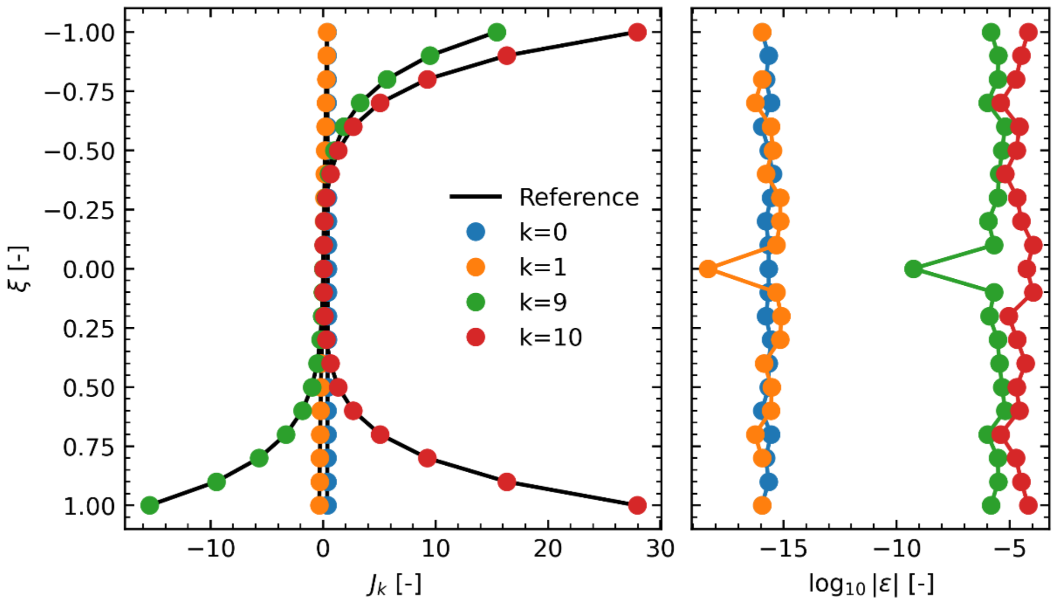

Figure 4. High-order integrals J_k evaluated along the borehole at $r_p = L$: (left) values, and (right) absolute errors

3.3. High-order finite line source solutions (I_k)

Fig. 5 shows the values of the 0th, 1st, 9th and 10th order of the integral I_k evaluated along the borehole (i.e. at $r_p = r_b$). The reference values of the integral of Eq. (18) are evaluated using the adaptive 21-point Gauss-Konrod quadrature. As in the cases of the inner integral X_k and of the integral J_k, the absolute error increases at higher orders. The absolute error at the borehole mid-point is $|\varepsilon| = 9.43 \cdot 10^{-5}$ when $k = 10$ and $I_{10} = 0.0935$. Since, the finite line source solutions are obtained simply from the binomial formula of Eq. (11), the absolute error remains of similar order of magnitude to the absolute error on the integral J_k.

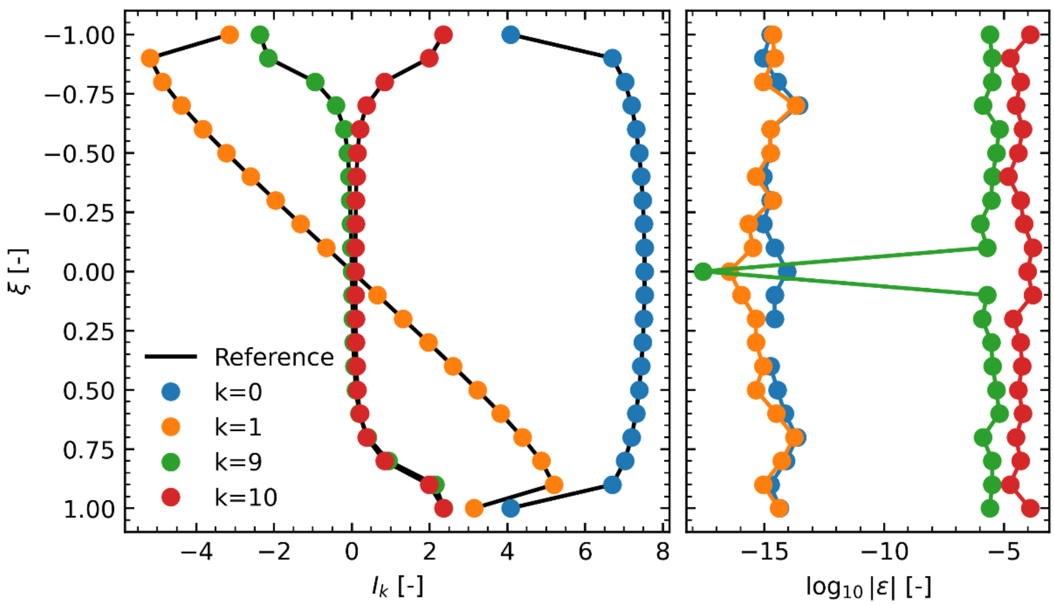

Figure 5. High-order finite line source solutions I_k evaluated along the borehole at $r_p = r_b$: (left) values, and (right) absolute errors

3.4. Thermal response factors (h_m)

Fig. 6 shows the thermal response factors of a borehole discretized using 11 nodes, located at coordinate ξ_m corresponding the locations of the roots of the Legendre polynomial of degree $n = 11$. Thermal response factors are evaluated at $\ln(t/t_s) = 5$, at positions corresponding to the longitudinal positions $s_b(\xi_m)$ of the nodes and at a radial distance $r_p = r_b$. Thermal response factors are shown for the impact of the first, center and last nodes along the boreholes (i.e. at $m = 0$, 5, and 10). These nodes were chosen since the edge nodes (i.e. $m = 0$ and 10) have the smallest errors and the center node ($m = 5$) has the largest errors. The maximum absolute error is $|\varepsilon| = 1.48 \cdot 10^{-2}$ at the mid-point when $m = 5$ and $h_5(\xi_5) = 5.53$ and the corresponding relative error is $|\varepsilon|/h_m = 2.69 \cdot 10^{-3}$. The relative error is much larger when evaluated at an edge node. For instance, the absolute error is $|\varepsilon| = 9.96 \cdot 10^{-3}$ at coordinate ξ_0 when $m = 5$ and $h_5(\xi_0) = 0.033$ and the corresponding relative error is $|\varepsilon|/h_m = 0.433$.

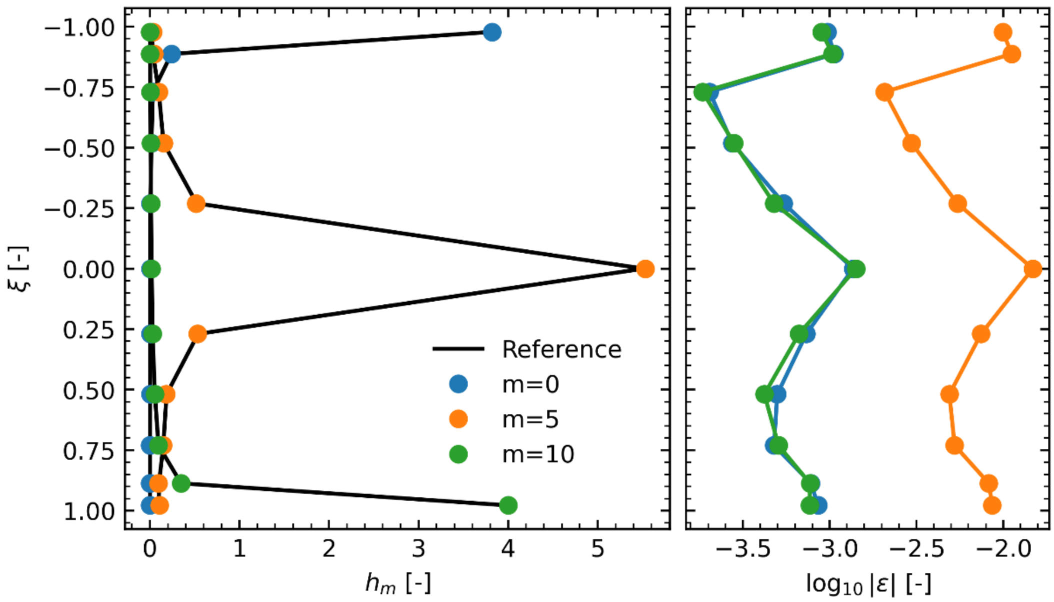

Figure 6. Thermal response factors h_m evaluated at nodes along the borehole at $r_p = r_b$: (left) values, and (right) absolute errors

4. Conclusions

A specialized solution for the high-order finite line source solution was presented. The solution uses a recurrence formula to evaluate the k^{th} order solution from the 0^{th} (for even k) or the 1^{st} order solution (for odd k), with only the 0^{th} order finite line source solution necessitating the numerical evaluation of an integral.

High-order finite line source solutions are shown to be correctly evaluated when compared to reference solutions. However, results show numerical errors that increase with the order of the finite line source solution, likely due to high powers that appear in the recurrence formula and to the sum of terms with alternating signs arising from the integration by parts. Greater numerical errors are observed when evaluating thermal response factors. The relative error is especially large at low values of thermal response factors. While the error is relatively large in these cases, it is not necessarily the case that these errors will translate into equally large errors in simulations or in the evaluation of g-functions, since the absolute error may remain small when compared to the total temperature change at nodes along the borehole. Future work will quantify the accuracy of the proposed specialized solution in the context of simulations and g-function evaluation.

Methods to decrease the numerical errors in the evaluation of the recurrence formula will also be explored. Potential solutions are to unroll the recurrence formulas of Eqs. (21) and (24) and evaluate the high degree polynomials using Horner's method, to develop an approximation for the high-order finite line source solution (for large k) and apply the recurrence backwards, or a combination of both.

5. Nomenclature

a_k : Coefficients for the polynomial representation of $q'(\xi)$
b_k : Coefficients for the polynomial representation of $q'(\eta)$
$c_{m,k}$: Basis function coefficients to evaluate thermal response factors from the finite line source solution
$h_m(\vec{p}, u)$: Thermal response factor of node m onto point $\vec{p}$
$I_k(\vec{p}, t)$: Finite line source solution of order k at point $\vec{p}$
$J_k(\vec{p}, t)$: Integral of order k at point $\vec{p}$

L : Length of the borehole
$\vec{p}$: Point (x, y, z)
$\hat{\vec{p}}$: Mirrored point $(x, y, -z)$
$\vec{p}_0$: Position of the head of the borehole (x_0, y_0, z_0)
$\vec{p}_b(\xi)$: Position along the borehole as a function of the coordinate ξ
$q'(\xi)$, $q'(\eta)$: Heat extraction rate per unit borehole length as a function of the coordinates ξ or η
r_p : Radial distance between point $\vec{p}$ and the axis of the borehole
$s_b(\xi)$: Longitudinal position along the borehole as a function of the coordinate ξ
s_p : Longitudinal position of point $\vec{p}$ projected onto the axis of the borehole
$\Delta T(\vec{p}, t)$: Temperature drop at point $\vec{p}$ due to heat extraction along the borehole
t : Time
u : Integration variable
$\vec{u}$: Unit vector for the orientation of the borehole, directed from top to bottom
$X_k(\vec{p}, u)$: Inner integral of order k at point $\vec{p}$
α : Ground thermal diffusivity
$|\varepsilon|$: Absolute error
η : Coordinate along the borehole axis, centered around the projection of point $\vec{p}$ onto the borehole
λ : Ground thermal conductivity
ξ : Coordinate along the borehole, with $\xi = -1$ at the top and $\xi = 1$ at the bottom

Acknowledgements

The authors acknowledge the support of the Natural Sciences and Engineering Research Council of Canada (NSERC), [funding reference number RGPIN-2025-04991]. The authors also acknowledge Energimyndigheten (Swedish Energy Agency) for financing this research via the grants P2022-00486, P2022-00499 (TERMO program) and P2022-01040 (JPP SES and GEOTHERMICA ERA-Net network programs).

References

[1] Eskilson P., 1987. Thermal analysis of heat extraction boreholes, Ph.D. thesis, University of Lund.
[2] Zeng HY, Diao NR, Fang ZH. A finite line-source model for boreholes in geothermal heat exchangers. *Heat Transfer–Asian Research* 2002:**31**(7):558–567.
[3] Lamarche L, Beauchamp B. A new contribution to the finite line-source model for geothermal boreholes. *Energy and Buildings* 2007;**39**(2):188–198.
[4] Claesson J, Javed S. An analytical method to calculate borehole fluid temperatures for time-scales from minutes to decades. *ASHRAE Transactions* 2011;**117**(2):279–288.
[5] Cimmino M, Bernier M. A semi-analytical method to generate g-functions for geothermal bore fields. *International Journal of Heat and Mass Transfer* 2014;**70**:641–650.
[6] Cimmino M. The effects of borehole thermal resistances and fluid flow rate on the g-functions of geothermal bore fields. *International Journal of Heat and Mass Transfer* 2015;**91**:1119–1127.
[7] Zanchini E, Zanchini F. A fast and accurate semi-analytical method to determine the thermal response of bore fields. *Science and Technology for the Built Environment* 2025;**0**:1-18.
[8] Lazzarotto A. A methodology for the calculation of response functions for geothermal fields with arbitrarily oriented boreholes — part 1. *Renewable Energy* 2016;**86**:1380–1393.
[9] Cui P, Yang H, Fang Z. Heat transfer analysis of ground heat exchangers with inclined boreholes. *Applied Thermal Engineering* 2006;**26**(11):1169–1175.
[10] Marcotte D, Pasquier P. The effect of borehole inclination on fluid and ground temperature for GLHE systems. *Geothermics* 2009;**38**(4):392–398.
[11] Lamarche L, Analytical g-function for inclined boreholes in ground-source heat pump systems. *Geothermics* 2011;**40**(4):241–249.
[12] Cimmino M, Basquens M, Lazzarotto A. Higher-order semi-analytical model for the simulation of geothermal boreholes. *International Journal of Thermal Sciences* 2026;**219**:110184.
[13] Harris CR, Millman KJ, van der Walt SJ, et al. Array programming with NumPy. *Nature* 2020;**585**:357–362.
[14] Virtanen P, Gommers R, Oliphant, TE, et al. SciPy 1.0: Fundamental Algorithms for Scientific Computing in Python. *Nature Methods* 2020;**17**(3):261–272.